Journal of Membrane Science & Research

journal homepage: www.msrjournal.com

Research Paper

Formation of SAN Nanofibrous Membranes Using DMSO Solvent with Low Toxicity for MD Process

Ali Sallakh Niknejad [1, *], Mohammad Pishnamazi [2], Saeed Bazgir [1, 3, *], Ali Kargari [4, *], Mohammad Mahdi A. Shirazi [5], Mohsen Rasouli [6]

[1] *Nano polymer Research Laboratory (NPRL), Science and Research Branch, Islamic Azad University, Tehran, Iran*
[2] *Chemical and Petroleum Engineering Department, Sharif University of Technology, Tehran, Iran*
[3] *Department of Polymer Engineering, Petroleum, and Chemical Engineering Faculty, Science and Research Branch, Islamic Azad University, Tehran, Iran*
[4] *Membrane Processes Research Laboratory (MPRL), Department of Chemical Engineering, Amirkabir University of Technology (Tehran Polytechnic), Tehran, Iran*
[5] *Department of Chemical Engineering, University of Kashan, Kashan, Iran*
[6] *SEM Lab, Central Laboratory, Amirkabir University of Technology, Tehran, Iran*

Article info

Received 2023-03-05
Revised 2023-06-29
Accepted 2023-10-22
Available online 2023-10-22

Keywords

Membrane Distillation
Nanofibrous Membrane
Green Solvent
Styrene-acrylonitrile (SAN)
Hydrophobicity

Highlights

- DMSO solvent was used to fabricate eco-facile SAN ENMs.
- High-throughput ENMs fabricated by electroblowing.
- Cold-pressing was used to enhance overall performance.
- SAN/DMSO ENMs were systematically evaluated and compared.
- Superior flux and comparable salt rejection compared to the PTFE one.

Graphical abstract

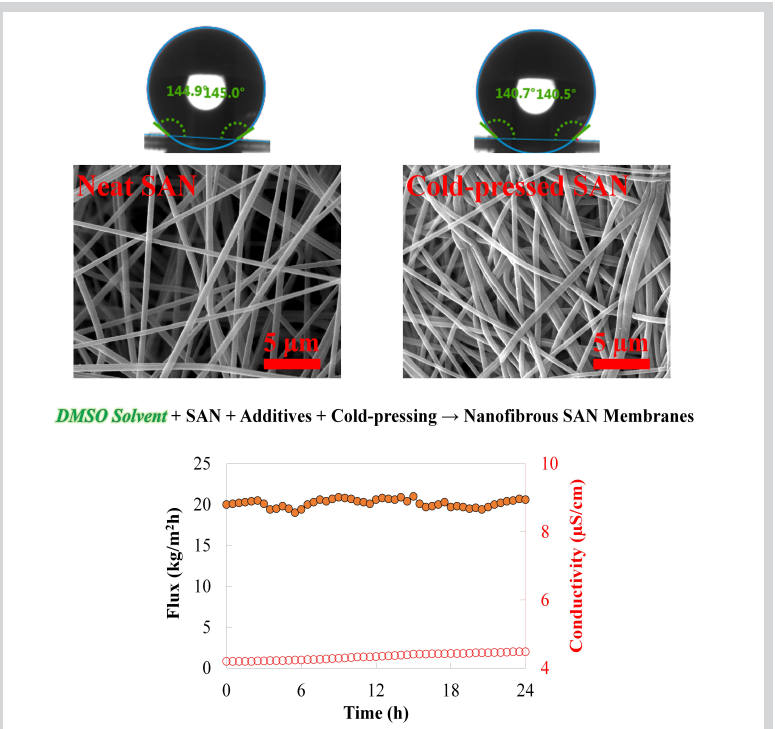

Abstract

Electrospun membranes have a significant share in membrane separation technology, especially in the membrane distillation (MD) process. However, not only hazardous solvents have been used to prepare hydrophobic nanofibrous membranes but also productivity is not satisfactory. Hydrophobic nanofibrous membranes were therefore proposed using dimethyl sulfoxide (DMSO) as an eco-friendly solvent, an electroblowing process as a high-productive process, and styrene-acrylonitrile (SAN) polymer as a cost-effective membrane material. The cold-pressing was used to enhance the membrane robustness. Membrane characteristics and direct contact membrane distillation (DCMD) performance of the SAN/DMSO and SAN/dimethylformamide (DMF) membranes were compared with a commercial polytetrafluoroethylene (PTFE) membrane. Compared to the commercial PTFE membrane, better permeation, and comparable salt rejection (>99.9%) were achieved for the cold-pressed SAN membranes when 35 g/L NaCl was used as the feed. This study showed that the DMSO solvent could be an alternative for limiting the use of common toxic solvents for fabricating hydrophobic nanofibrous membranes with competitive performance.

* Corresponding authors: aliniknejad1991@gmail.com (A. S. Niknejad), bazgir@srbiau.ac.ir (S. Bazgir), kargari@aut.ac.ir; ali_kargari@yahoo.com (A. Kargari)

DOI: 10.22079/JMSR.2023.1990984.1593

1. Introduction

Polymeric membranes are high-tech products that have found many applications in industry and domestic [1]. Among the membrane fabrication methods, electrospinning has attracted much attention because through this method membranes with unique properties could be fabricated, say ease of nanofiber production, higher porosity, adjustable pore size, higher surface-to-volume ratio, better functionality, and so on [2]. The electrospinning process has been considered a capable method for fabricating polymeric nanofibers with different sizes varying from some nanometers up to micron size [3]. Due to its unique properties including high surface-to-volume ratio, high porosity, fabricating nanofibers from a wide range of polymers, and so forth, this method was successfully implemented in different fields. Membranes [4], wound dressing [5], drug delivery [6], and so on are the objective points for the electrospun nanofibers. Normally, 70 to 90 weight percent of polymeric dope solution for the fabrication of the membranes are solvents. However, electrospinnable polymers like polystyrene (PS) [7], polyacrylonitrile (PAN) [8], polyvinylidene fluoride (PVDF) [9], polysulfone (PSU) [10], and cellulose acetate (CA) [11] are not soluble in water. These polymers dissolve in aprotic and regular organic solvents that are used in electrospinning processes such as *N,N*-dimethyl acetamide (DMA) [12], *N,N*-dimethylformamide (DMF) [13], tetrahydrofuran (THF) [14], and acetone [15]. Nevertheless, these solvents are harmful to the environment and the human body itself. Fabricating membranes using these solvents is a secondary source of pollution.

The application of environmentally friendly routes for the fabrication of membranes is a way of limiting or eliminating toxic solvent release during the membrane fabrication process. Dimethyl sulfoxide (DMSO) is an organic and highly polar solvent able to dissolve a wide range, from water-soluble to water-insoluble polymers [16,17]. DMSO is extracted from lignin or can be produced by the oxidation of dimethyl sulfide. DMSO is a low-toxic and biodegradable solvent creating non-toxic products [18,19]. Table 1 lists hazard statements of the mentioned solvents. Compared to highly toxic solvents, the more sustainable route for membrane fabrication has rarely been investigated. Coupling a less toxic membrane fabrication procedure with membrane-based separation processes having a low carbon footprint is of great importance. Membrane distillation (MD) is a promising process that has some great potential to be commercialized for producing potable water from saline and seawater. This process can be coupled with renewable energy sources like solar, wind power, and waste-heat sources from thermal-including processes [20].

Table 1
Hazard statements for the typical solvents used in membrane fabrication processes [17].

Solvent	Hazard statement
NMP	H315, H319, H335, H360D
DMA	H312, H332, H319, H360D
DMF	H226, H312, H332, H319, H360, H360D
THF	EUH019, H225, H302, H319, H335, H351
DMSO	Not a hazardous substance or mixture
NMP: 1-methyl-2-pyrrolidinone. H225: Highly flammable liquid and vapor. H226: Flammable liquid and vapor. H302: Harmful if swallowed. H312: Harmful in contact with skin. H315: Causes skin irritation. H319: Causes serious eye irritation.	H.332: Harmful if inhaled. H335: May cause respiratory irritation. H351: Suspected of causing cancer. H360: May damage fertility or the unborn child. H360D: May damage the unborn child. EUH019: May form explosive peroxides.

MD process is the combination of the distillation and membrane separation process. The membrane used in this process should be hydrophobic enough only to provide a passage for the water vapor instead of the liquid feed [21]. The mass transfer through the membrane is governed by the partial pressure difference of water vapor at the two sides of the membrane that depends on the temperature differences between the two sides of the membrane [22,23]. MD process operates at low to moderate temperatures (between 40 and up to 80 °C), has a high salt rejection, is less affected by the feed concentration, and is less sensitive to the membrane's mechanical properties than the pressure-driven process [24,25]. To date, the MD process has been used extensively for treating a wide range of wastes from pharmaceutical [26], textile, and dying wastes [27,28], radioactive waste [29,30], seawater [31] to synthetic saline water [32]. However, the MD process suffers from the pore-wetting phenomenon, low permeate flux, and the lack of suitable design for MD modules [33-35].

Commercial membranes are the common contributors in MD processes that are initially designed for the microfiltration process. The main reasons that impede the commercialization of these membranes are low hydrophobicity (hardly reaches 130°), high expenses originating from expensive polymeric raw materials like PVDF and polytetrafluoroethylene (PTFE), and expensive fabrication processes [36,37]. Particular attention should be paid to using highly toxic and harmful solvents like strict wastewater and air treatments, recycling, and reuse, and labor exposure which in turn increases the production costs. From this point of view, the application of less toxic solvents in conjunction with a facile fabrication method enhances membrane productivity and reduces production costs simultaneously.

The electroblowing technique is an upgraded mode of the typical electrospinning process offering a better fiber production rate than regular electrospinning [38]. In this technique, compressed dry air is introduced into a coaxial needle, forms a continuous jet of the polymeric solution, and the resulting fibers are deposited on a rotating collector. Moreover, electroblowing owns all the highlighted characteristics of the electrospinning process for membrane fabrication. The spinning speed of this process is much higher than that of the reported works (5-30 µL/min) for fabricating nanofibrous MD membranes by using electrospinning. In our earlier publications for fabricating nanofiber PS [39], high-impact PS/styrene-acrylonitrile (SAN) [40], and SAN [41] MD membranes using the electroblowing process, the outstanding spinning speed of 117, 135, and 270 µL/min were used, respectively, which means higher productivity and most importantly can be translated into sufficient use of time.

The electrospinning process relies on varied parameters including polymer concentration, viscosity, tip-to-collector distance, applied voltage, conductivity, and boiling point (b_p) of the solvent to name a few. To produce a fine and defect-free nanofibrous layer using available polymers, a set of parameters should be adjusted. The characteristics of the applied solvent system to make an electrospinning solution are of immense importance. Generally, two factors should be considered before making a spinning solution that is the solubility of the target polymer in the solvent and moderate volatility. b_p and vapor pressure define solvent volatility. Considering the electrospinning process, a proper solvent system must neither have a high boiling point nor a very low boiling point. A spinning solution with very low b_p will make the polymeric solution block the needle due to the fast evaporation of the solvent. Also, using a solvent with a lower b_p will cause some defects since a considerable amount of solvent remains inside the formed structure. Apart from the volatility of the employed solvents, solvent conductivity also has a considerable effect on the final morphology of the formed fibrous structure as a spinning solution having low or non-conductive character will not respond to the applied electrical field to form a constant jet of fibers [42,43]. Solvent selection is even more vital for the electroblowing process because of the employment of dry air flow. Due to the application of needle electroblowing to fabricate nanofibrous membranes, needle blockage should be handled properly.

In the present work, hydrophobic nanofibrous membranes are fabricated using SAN as an inexpensive and readily available polymer, electroblowing technique as a high-output membrane fabrication process, and DMSO as a less toxic solvent. To better understand the influence of DMSO on the properties and separation performance of nanofiber membranes, similar membranes were fabricated using the DMF solvent. These two types of membranes are characterized and applied for desalination in the direct contact membrane distillation (DCMD) process using synthetic salty water (35 g/L) and the results are compared to that of PTFE membrane as well as existing literature using electrospun membranes. As far as we know, it is the first study using a low-toxic DMSO solvent to fabricate nanofibrous MD membranes.

2. Materials and methods

2.1. Chemicals

Commercial grade SAN, SAN-4, was provided by Gaed-Basir Petrochemical Company, Iran. DMSO, DMF, and acetone were supplied from Ameretat Shimi (TAT chem), Iran. Analytical grade NaCl and isopropyl alcohol (IPA) were purchased from Dr. Mojallali Co, Iran. cetyltrimethylammonium bromide (CTAB) was bought from Merck, Germany.

A commercial PTFE membrane with 0.22 µm pore size and thickness of 180 µm (20 µm PTFE layer mounted on polypropylene (PP) support layer) was provided by Membrane Solutions, LLC.

Table 2
System and operational conditions of electroblowing process for fabricating neat SAN membranes.

Code	Concentration (wt.%)	Voltage (kV)	Injection rate (μL/min)	Working distance (cm)	Time (min)	Airflow rate (NL/min)
S-1	20 (DMF/acetone)	21	270	30	60	3
S-2	20 (DMSO)	21	270	30	60	3
S-3	20 (DMSO)	24	270	30	60	4.5
S-4	20 (DMSO/acetone)	21	270	30	60	3

2.2. Membrane preparation

The laboratory-scale electroblowing setup was depicted elsewhere [44]. 20 wt.% of SAN granules were dissolved in a DMF/acetone mixed solvent system (70:30). To make DMSO-containing spinning solutions, 20 wt.% SAN was dissolved in pure DMSO and DMSO/acetone (70:30). A small amount of CTAB salt was added to all spinning solutions to increase conductivity (0.25 wt.% considering polymer weight). After complete dissolution, the resultant solutions were stood overnight for degasification. Then the solutions were electroblown under the conditions taken in Table 2. A 20 mL syringe was filled with the dope solution connected to a syringe pump (SP100HSM, FNM, Iran). The electrical field was supplied by an adjustable power supply. A coaxial spinning needle consisting of two concentric needles (19 G and 14 G) was connected to the syringe via a PP tube. Dry compressed air was supplied by an air compressor (MK160, FINI, Italy) and a silica gel bed. Before the electroblowing, the surface of the rotating drum was covered with a nonwoven PP mat as the collecting surface. Fabricated neat membranes were identified by S-x (i.e., S-1, S-2, S-3, and S-4) codes.

The fabricated nanofibrous SAN membranes were then cold-pressed (2000 psi and 10 s) to obtain a uniform and flat fibrous structure. The cold-pressed membranes were named CS-x (i.e., CS-1 means cold-pressed S-1 membrane). After cold-pressing the membranes, the PP nonwoven mat was removed and then the characterization and evaluation of the fabricated membranes were performed.

2.3. Membrane characterization

The surface morphology of the used membranes in this study was observed using a scanning electron microscope (SEM; AIS2300C, Seron Technology, Korean Republic). The membrane samples were coated with a thin layer of gold and then transferred to the SEM vacuum chamber.

The SEM images are then processed by Digimizer software to measure and report the average diameter of fibers and surface pore size [45,46].

The thickness of the membranes was measured by a digital thickness gauge (OSK 11334, Japan; 0.001 mm resolution). The average of five different measurements was then reported.

The porosity of the membranes was determined using the gravimetric method [47]. The membrane samples (3×3 cm^2) were weighed before and after immersing in IPA.

To get the stress-strain curves, 1×5 cm^2 strips were cut and tested by a tensile machine (Instron Dynamometer, model 5566) using a 50 N load and a stretching speed of 5 mm/min. All tests were conducted at ambient conditions.

The hydrophobicity of the membrane surface was evaluated by a water droplet contact angle measuring apparatus (KRUSS analyzer-G10 Drop Shape Analyzer, Germany). The membrane sample was first fixed on the device holder using two glass slides and then 2 μL deionized water (DI water) was gently dropped on the membrane surface and the water contact angle (CA) was calculated by the respective device software.

The liquid (water) entry pressure (LEP) of the membranes was measured using a homemade device that has been described in detail elsewhere [48].

2.4. DCMD test

For the evaluation of the performance of the studied membranes, a laboratory-scale DCMD system was used. The representative schematic of this system is shown in Fig. 1. A DCMD module made of polyethylene (effective area, 5×2.5 cm^2) was used. DI water (~ 4.2 μS/cm) was used as the initial permeate liquid. Four temperature sensors were applied to monitor the inlet and outlet temperatures. The temperature of the feed and the permeate streams was fixed at 55 and 15 ºC, by an electric heater and a water chiller, respectively. The flow rate for the feed and the permeate streams were maintained at 0.48 and 0.24 L/min, respectively, using two peristaltic pumps. Also, feed temperature/flow rate effects on DCMD performance were assessed. A conductivity meter (Metrohm-912, Switzerland) was used for measuring the electrical conductivity (EC) of the feed and permeate samples. The feed concentration (35 g/L NaCl) was kept constant by periodically monitoring and regulating the concentration.

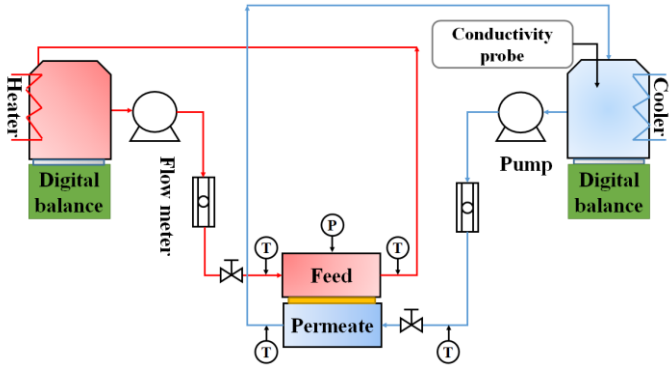

Fig. 1. The experimental DCMD set-up.

3. Results and discussion

3.1. Morphology

Fig. 2 shows the SEM images of the neat and cold-pressed SAN membranes as well as the PTFE membrane. The average fiber diameter for the S-1 membrane was lower than that of the membranes fabricated by either DMSO solvent or DMSO/acetone solvents due to the application of different solvents and electroblowing conditions. Russo et al. [49] fabricated DMF/acetone/PVDF and DMSO/acetone/PVDF nanofibrous layers with different concentrations. The fiber diameter of the DMF/acetone/PVDF nanofibers was lower than that of the latter. DMSO solvent is more conductive than DMF solvent (DMSO dielectric constant, 46.7; DMF dielectric constant, 37.3 [50]). Also, the addition of CTAB salt further increased the conductivity of the DMSO-including spinning solutions resulting in an enhancement in fiber diameter. The same phenomenon was observed by adding 3 droplets (~15 μL) of nitric acid into the DMF/HIPS spinning solution with 20 wt.% concentration (spinning solution weight of 30 g). Fig. 3 shows the obvious increase in fiber diameter after increasing the conductivity of the spinning solution. Faster solvent evaporation or an increase in the deposition speed of nanofibers in contact with an electrical field may be the reasons for to increase in fiber diameter. As DMSO solvent has a higher boiling point than DMF (189 versus 153 ºC), under the same electroblowing condition, the fibers resulting from DMSO solvent have less intention for losing the solvent and becoming dry; therefore, only the surface of the fibers dry fast while the inner parts of the fibers are still wet. So, it can cause undesirable fiber fusion without any processing, forming non-uniformity throughout the nanofibrous network, as evident by the SEM image of the S-2 membrane. In this situation, the fibers experienced less shrinkage upon drying and the resultant fibers have larger diameters than the fibers resulting from DMF as the solvent. Such a discussion could be made for another reason the difference between the mean fiber diameter of the S-2 and CS-2 membranes (see Table 3). As the fibers are collected on the surface of the collector, the higher spinning times cause the non-completely dried fibers to be piled on each other and the evaporated solvent from the fibers accumulates between the nanofibers and lowers the mass transfer driving force for the solvent evaporation, therefore the shrinkage of the nanofibers decrease, and the final fibers diameter increases. To overcome the mentioned problems, two approaches were employed. First, to facilitate the evaporation of the remaining solvent inside the fibrous structure, higher applied voltage and airflow were used; thus, a larger fiber diameter was created. For the second solution, acetone solvent was used to facilitate solvent evaporation and decrease the undesirable effect of fiber diameter enhancement. These two simple strategies have well restricted the loss of hydrophobicity due to fiber diameter increment (extra surface roughness reduction) after cold-pressing, as the mean fiber diameter of the cold-pressed SAN membranes (except for CS-2) remained constant. By further increasing acetone concentration, the fiber diameter of the formed DSMO/acetone/SAN nanofibers was increased

progressively, even when SAN concentration (12.5 wt.%) was reduced to partly neutralize the fiber diameter enhancement phenomenon. Fig. 4 shows the SEM images for the SAN nanofibers made of DMSO/acetone (1:1) using the same electroblowing conditions. The needle blockage was also observed by adding a higher amount of acetone to the spinning solution since acetone has a very low b_p compared to the DMSO solvent making the spinning solution more susceptible to earlier polymer/solvent solidification.

Furthermore, the inter-fiber space of all nanofibrous SAN membranes experienced considerable reduction after the cold-pressing process due to extra compaction imposed by the pressing process. The cold-pressed SAN membranes enjoy having improved LEP (reduced pore size), better mechanical robustness, and boosting permeate flux due to substantial thickness reduction and suffer from reduced porosity and hydrophobicity. These pros and cons were investigated in detail in the next sections.

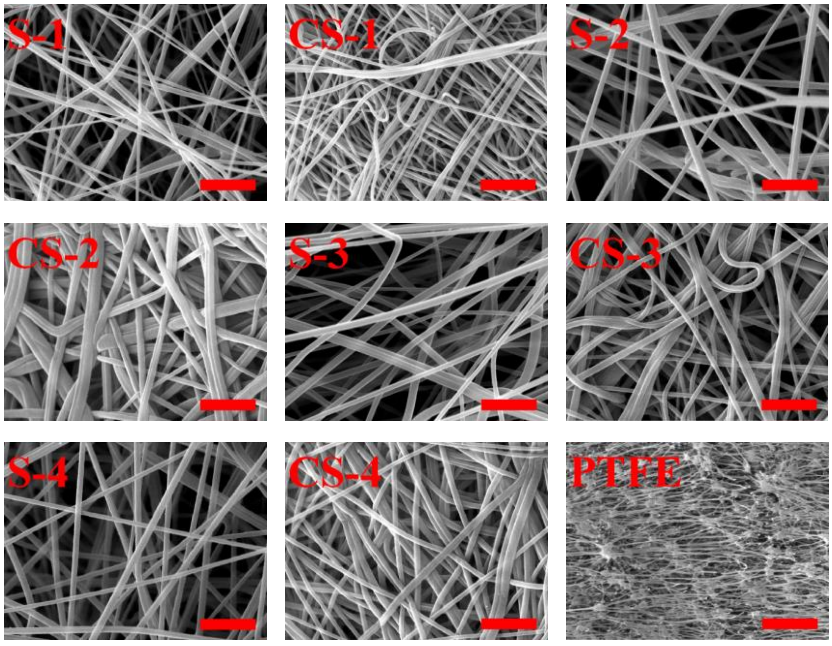

Fig. 2. Surface morphology of the employed membranes in this work. The red scale-bar is 5 µm.

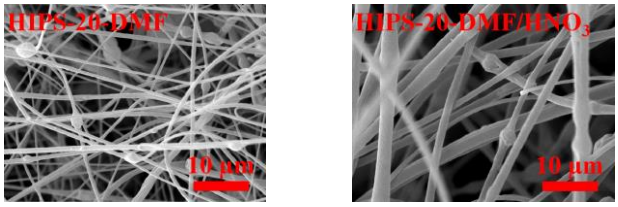

Fig. 3. SEM images for the HIPS nanofibers formed using DMF solvent and HNO_3 as additive.

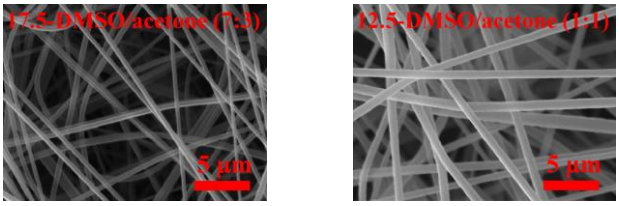

Fig. 4. Surface morphology for the SAN nanofibers fabricated using different conditions.

Table 3
Characteristics of the studied nanofibrous and PTFE membranes.

Code	d_f (nm)	δ (µm)	ε (%)	WCA (°)	r_{mean} (µm)	r_{max} (µm)	LEP (kPa)
S-1	324 ± 91	895 ± 60	98.6 ± 1	146.2 ± 1	0.52 ± 0.02	1.87 ± 0.03	64.3 ± 2
CS-1	310 ± 68	167 ± 3	82.3 ± 1	141.1 ± 1	0.27 ± 0.01	0.56 ± 0.01	217.2 ± 1
S-2	532 ± 72	1240 ± 70	97.2 ± 2	144.9 ± 1	0.73 ± 0.03	2.25 ± 0.04	50.4 ± 3
CS-2	635 ± 171	190 ± 2	73.2 ± 1	134.7 ± 1	0.38 ± 0.01	0.79 ± 0.02	148.3 ± 1
S-3	606 ± 78	1420 ± 50	97.6 ± 2	144.5 ± 1	0.85 ± 0.01	2.61 ± 0.05	53.2 ± 2
CS-3	580 ± 64	195 ± 4	81.3 ± 1	139.8 ± 1	0.43 ± 0.03	0.91 ± 0.03	166.3 ± 1
S-4	451 ± 82	1160 ± 45	98.8 ± 1	145.7 ± 1	0.59 ± 0.02	2.12 ± 0.04	67.2 ± 2
CS-4	463 ± 56	179 ± 2	82.7 ± 1	141.8 ± 1	0.32 ± 0.01	0.66 ± 0.02	202.4 ± 1
PTFE	115 ± 51	180 ± 2	72.6 ± 3	128.6 ± 1	0.24[1] ± 0.01	0.53 ± 0.01	127.7 ± 1

Fiber diameter, d_f; thickness, δ; porosity, ε; water contact angle, WCA; mean pore size, r_{mean}; maximum pore size, r_{max}; liquid entry pressure of water, LEP.
[1] Measured by surface analyzing program.

3.2. Thickness

The performance of a membrane (separation factor, flux, and fouling characteristics) results from different factors from the selection of membrane material and solvent to the fabrication method and post-treatment processes applied on the final membrane. In nanofibrous membranes, which are a type of depth filter, membrane thickness greatly impacts the flux and particle retention. Previous studies have shown that membrane thickness could affect the mechanical properties, wetting characterizations, and LEP of the final membrane. As the flux of the thicker membranes is much lower than the thinner membranes, the thinner membranes are more favorable. On the other hand, the thin membranes are not mechanically strong enough, wetted easily (have lower LEP), and have high heat loss that is not suitable for membrane distillation applications. The previous investigations on finding suitable membranes for MD applications show that the thicker membranes exhibit better performance for desalination of high salinity waters, whereas thinner membranes have higher performance for low salinity feeds like brackish waters [51].

In Table 3, the characteristics of the fabricated SAN membranes are shown. The results demonstrate that the neat SAN membranes have larger thicknesses compared to the cold-pressed membranes. Typically, the membranes that are fabricated by the electroblowing method have greater thicknesses than membranes fabricated by the traditional electrospinning method due to the formation of a thicker layer of fibers on the collector and the fading of the effect of the applied electrical field during the spinning process. Based on our experience, removing the formed nanofibrous layer from the PP support is much easier than using a thin aluminum foil as the collecting surface. Therefore, using PP nonwoven collecting surface as an insulation for the proper deposition of the electrical charge and the effect of thickness enhancement makes a more porous and loose nanofibrous structure [48]. As shown in Table 3, applying cold-pressing on the SAN membranes has decreased pore size and membrane thickness considerably, while at the same time increasing the membranes' mechanical strength (see Table 4). At that point, cold-pressing the neat SAN membranes not only decreased the potential of pore wetting by the process liquids but also reduced the mass transfer resistance for vapor transport through the membrane thickness.

Table 4
Mechanical properties of the fabricated and PTFE membranes.

Code	Stress at break (MPa)	Elongation at break (%)
S-1	1.40	17.31
CS-1	7.17	12.93
S-2	1.97	18.61
CS-2	9.50	12.91
S-3	2.17	20.16
CS-3	11.42	11.42
S-4	1.75	24.13
CS-4	8.99	15.62
PTFE	19.32	10.21

3.3. Wetting resistance

According to the Laplace formula ($LEP=-\beta\gamma_l\cos\theta/r_{max}$), LEP is the pressure of a liquid (mainly water) in which the liquid penetrates through the membrane and corresponds to the largest pore. The formula shows that LEP depends directly on the surface geometry factor of β, liquid-solid interfacial tension γ_l, and the cosine of the angle between the solid surface and liquid droplet and inversely to the pore radius. LEP is a good criterion for pore wetting tendency in a membrane taking into account the characteristics of the surface, liquid properties, and surrounding atmosphere at the same time, so the lower LEP shows more susceptibility for wetting by the process liquid.

In Table 3, the measured water droplet contact angle, WCA, was tabulated for the studied membranes. All the neat membranes have contact angles greater than 140° except for the PTFE membrane. However, the contact angle shows a reduction after cold-pressing due to a reduction in the surface fiber roughness [52]. As mentioned before, enhancing the fiber diameter of the CS-2 membrane was expected due to the entrapped solvent inside the nanofibers and it can cause an extra reduction in surface hydrophobicity compared to the other cold-pressed SAN membranes.

For the commonly used materials for MD membranes like PTFE, PVDF, and PP that all are hydrophobic enough for the MD application, pore size plays a vital role in the corresponding membrane pore wetting. The larger pores are more susceptible to pore wetting and the smaller pores have lower vapor permeation flux. According to the literature, pore sizes in the range of 0.1 up to 1.0 µm and mostly in the range of 0.2 to 0.5 µm are recommended for MD application [53]. As mentioned earlier, r_{max} has a key role in the determination of LEP value; therefore, it must be as close to the average pore size as possible to limit pore wetting. Fortunately, after cold-pressing, both the mean and maximum pore sizes were reduced. The pore size of the as-prepared membranes was placed in the range of 0.52 - 0.85 and 1.87 - 2.61 µm, for the mean pore size as well as maximum pore size, respectively, whereas for the cold-pressed SAN membrane, these values were in the range of 0.27 - 0.43 and 0.56 - 0.91 µm. Consequently, a proper conclusion can be drawn that the cold-pressed membranes are more resistant to pore wetting than the corresponding neat membranes. Although the reported LEP values for the commercial flat-sheet MD membranes, depending on membrane material and fabrication method, are in a broad range from 48 to 463 kPa [14], according to the literature, LEPs higher than 200 kPa are appropriate for MD applications to ensure long term performance [40]. The results of Table 3 reveal that the LEP value for the SAN membranes has increased considerably after cold-pressing up to 217.2 kPa.

3.4. Porosity

A membrane with high porosity provides a higher void volume for fluid transport across the membrane through the pores. In a better word, higher porosity results in higher permeate flux. In the MD process, high porosity would reduce heat loss across the membrane since thermal conductivity for the high porosity membrane is much lower than both the polymer and liquid feed [22]. On the other hand, the increase in porosity lowers the mechanical properties of membranes. The preferred range for porosity is reported in the range of 30 to 85% [54]. The porosity of the neat nanofibrous SAN membranes was higher than 97%. As mentioned before, the presence of high repulsion forces between the nanofibers during the fiber formation and collection results in a loose and soft nanofibrous structure with a high void volume. However, a considerable reduction in porosity was observed upon the cold-pressing of the neat membranes. Although cold-pressing has decreased the porosity (<83%, except for the CS-2), they are still acceptable for guaranteeing a successful MD operation. It needs to be stated that a bigger reduction of porosity for the CS-2 membrane comes from the residual solvent in/on the fibers making them more compact by forming fused nanofibers.

3.5. Mechanical characteristics

Due to the moderated operating condition of the MD process compared to the pressure-driven membrane-based processes, MD membranes should mostly endure packing stress and hydrostatic pressure imposed on the fibrous mat [55]. The mechanical behavior of nanofiber membranes has a close relationship with the polymer material property, membrane morphology, and structure [47]. The tensile strength of a nanofibrous membrane with a smaller fiber diameter is lower than that of a membrane having thicker fibers [56]. Essalhi and Khayet [57] reported that membrane thickness directly influences tensile strength since the thicker membrane is more robust than the thinner one. Stress-strain graphs for the as-prepared, cold-pressed, and PTFE membranes were presented in Fig. 5 and the corresponding data for stress at break and elongation at break were tabulated in Table 4.

As was expected, the neat SAN membranes have lower stress at the break than their corresponding cold-pressed samples (see Table 4). Higher porosity and looser fibrous structure are the leading causes of a weak membrane. After the cold-pressing, stress at the break of the membranes was increased considerably. Also, cold-pressed membranes experienced insignificant reductions in the strain at break. Given these attributes, cold-pressed membranes can exhibit better mechanical properties when facing the hot feed solution in long-term DCMD applications.

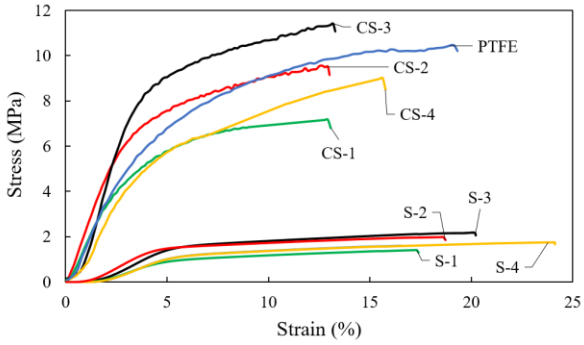

Fig. 5. Stress-strain diagram of the membranes used in this study.

3.6. DCMD performance

In this section, the DCMD performance of the cold-pressed nanofibrous and commercial membranes is investigated. Despite neat membranes having higher hydrophobicity and porosity, these membranes are not proper for DCMD operation because of lower mechanical and LEP values; therefore, only cold-pressed membranes were evaluated for the DCMD desalination process. Permeate flux-time diagrams are presented in Fig. 6.

After cold pressing, the thickness of all membranes reduced significantly, and the mechanical strength increased. At the same time, membrane pore size decreased considerably, reducing the probability of pore wetting, while the final pore sizes lay within the recommended pore size range for MD membranes. Cold-pressed membranes showed higher permeability over PTFE membranes due to higher hydrophobicity, higher porosity, and bigger mean pore size. Permeate flux for CS-1, CS-2, CS-3, CS-4, and PTFE membranes was measured as 16.86, 13.47, 22.65, 20.16, and 11.81 kg/m^2 h, respectively. Among the cold-pressed SAN membranes, CS-2 gained the least permeable membrane because of its inferior porosity and hydrophobicity and higher thickness than that of the CS-1 and CS-4 membranes.

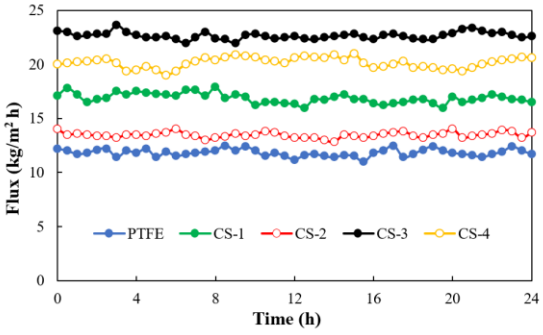

Fig. 6. Flux-time diagrams for cold-pressed SAN and PTFE membranes using 35 g/L synthetic salty water (ΔT = 40 ºC, 0.48 L/min feed and permeate flow rate for 24 h).

In the case of wetting resistance, all of the tested membranes showed a high salt rejection factor (>99.9%) with no pore wetting during the 24-hour DCMD operation. In our previous work [48], the hot-pressed SAN membrane was fabricated after 30 min electroblowing followed by hot-pressing (LEP, 64.4 kPa; thickness, 70 µm) and was used for desalination of the 35 g/L synthetic NaCl solution. DCMD operating condition was set to be ΔT = 60 ºC (feed temperature of 80 ºC and permeate temperature of 20 ºC) with 0.48 L/min feed flowrate and 0.24 L/min permeate flowrate. Partial pore wetting was detected, as the EC of the permeate solution started to rise after 17 h of the DCMD test. This pore wetting could happen because of these four reasons: higher driving force (higher temperature differences), relatively lower LEP value, higher imposed hydrostatic pressure in the feed side than in the permeate side, and also lower surface tension and viscosity for the feed solution having a higher temperature. Wang et al. [58] and Su et al. [59] reported that applying higher feed flow rates in the feed channel can accelerate wetting incidents for membranes having bigger pore sizes (potential pores). Also, as the WCA of hot feeds is lower due to changes in water surface tension and membrane surface morphology, the LEP value could be smaller for the feeds with higher temperatures. However, under the mentioned operating condition for the DCMD operation in this work, partial pore wetting with a sudden decline in the permeate flux was not observed. Permeate water quality in terms of EC was lower than 5 µS/cm for the cold-pressed and PTFE membranes (initial permeate conductivity was about 4.2 µS/cm).

3.7. Effect of operating condition on DCMD performance

Feed and permeate temperatures flow rates and feed salinity are the main factors influencing DCMD performance. Among them, feed temperature is the most important factor, and the temperature difference between feed and permeate, feed and permeate flow rates, and finally feed salinity are in the next steps [60]. As mentioned earlier, the pore-wetting phenomenon is more likely to happen when high hydrostatic pressure (higher than the permeate side pressure) is imposed by the feed on the membrane. If the LEP of the membrane is high enough, no considerable pore wetting is observed unless the membrane becomes less hydrophobic because of scale formation on the membrane surface. As the fabricated membranes (cold-pressed membranes) in this study had high LEP, we were not worried about pore wetting throughout the experiment period.

To investigate the effect of feed temperature and flow rate on the DCMD, the CS-4 membrane was subjected to different feed temperatures and flow rates. Feed temperature has a dominant effect on enhancing membrane flux by increasing the mass transfer driving force by increasing the feed vapor pressure. At constant permeate temperature (15 ºC) by increasing feed temperature from 45 to 75 ºC, permeate flux was enhanced from 15.57 to 32.33 kg/m^2 h (see Fig. 7-A).

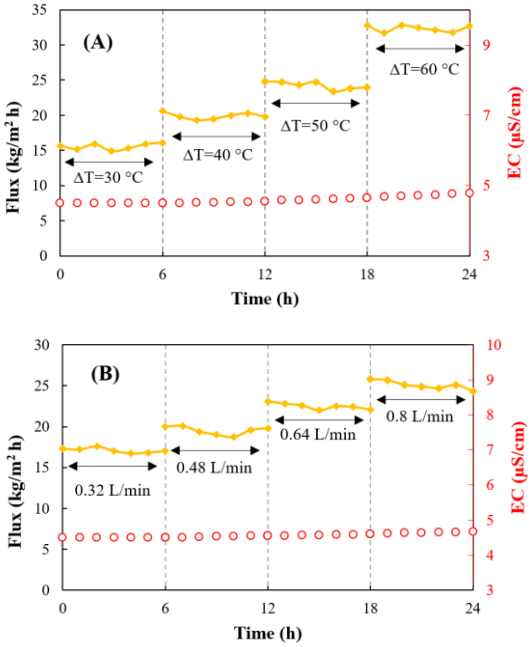

Fig. 7. Effect of (A) feed temperature and (B) feed flow rate on the permeate flux and EC of the permeate tank (Permeate temperature of 15 °C, feed concentration of 35 g/L NaCl, and permeate flow rate of 0.24 L/min).

Similarly, an increase in feed flow rate positively affects reducing polarizations (temperature and concentration polarizations) and maintains the feed-membrane interface temperature closer to the feed bulk temperature. A higher feed flow rate is beneficial for reducing the effect of a stagnant layer of salt on the membrane surface by forming turbulency which can lead to the limitation of salt deposition on the membrane surface. However, the effect of feed flow rate is not as significant as the effect of feed temperature in increasing membrane permeability. Fig. 7-B shows the flux-time diagram for the CS-4 membrane at different feed flow rates. It is worth quoting that salt retention was high (>99.9%) even after 24 h of DCMD operation.

3.8. Comparison of the results

Properties and performances of the recently used electrospun membranes for MD desalination are compared with the results of this work and summarized in Table 5.

This comparison reveals several promising achievements that can be attributed to the electroblown SAN membranes.

The nanofibrous SAN membranes possessed proper porosity compared to the electrospun nanofibrous membranes even after experiencing cold-pressing. Higher porosity lets water vapor pass through the membrane easier and a higher permeate flux is then achieved. Only hot-pressed membranes exhibited lower porosity than 80% as a result of higher structural compaction [48].

LEP value is the crucial factor for overall membrane robustness during long-term MD operation. As can be seen from Table 5, cold-pressed SAN membranes have the highest LEP among the others. Higher thickness, smaller maximum pore size, and suitable surface hydrophobicity are the main factors determining the final LEP value. Despite lower heat loss and more robust mechanical attributes for membranes with thicker structures, it has a negative effect on membrane permeability.

Cold-pressed SAN membranes exhibited almost complete salt rejection due to their high LEP value, high surface hydrophobicity, and considerable mechanical strength. During the 24-hour continuous DCMD desalination operation, the conductivity of permeate remained almost constant, emphasizing the superior performance of these membranes for desalination application.

Table 5
Properties and DCMD performance of different single-layer MD membranes by using 35 g/L NaCl as feed water.

Membrane	r_{mean} (µm)	δ (µm)	ε (%)	WCA (°)	LEP (kPa)	ΔT (°C)	Q_f (L/min)	t_p (h)	J_w (kg/m²h)	R (%)
PS-25 [13]	1.15	120	77.5	150.2	80	45	0.6	10	51	>99.9
PS-8-3 [7]	0.19	147	84	114	150	53	0.75	10	19.4	>99.9
SBS [14]	0.58	200	81	132	81	35	0.5	120	11.2	>99.9
10 PH-hotpress-2layers [61]	0.26	110	~60	~125	131.6	41	15	-	20-22[1]	~98
PH-20 [47]	0.76	87	88.6	143.5	65.8	~40	0.45	48	~40	>99
PVDF-3 [12]	1.04	847	87.5	142.5	89	60	500[2]	-	~50[3]	>99.9
PSF-3 [12]	1.88	564	89.3	138.7	29	60	500[2]	-	~33[3]	>99
PVDF [57]	3.6	144	86	139.7	~65	40	500[2]	-	17.3[3]	>99.9
EB60HP [39]	0.56	65	74	154	38.6	60	0.6	6	22.59	>99
SP-60 [48]	0.18	105	70.3	133.4	118.9	60	0.48	24	41.8	>99.9
CS-3 (this work)	0.43	195	81.3	139.8	166.3	40	0.48	24	22.65	>99.9
CS-4 (this work)	0.32	179	82.7	141.8	202.4	40	0.48	24	20.16	>99.9

Feed flow rate, Q_f; DCMD duration, t_p; permeate flux, J_w; salt rejection, R.
[1] 10 g/L.
[2] rpm.
[3] 30 g/L.

4. Conclusion

Electrospun polymeric membranes have been considered a viable alternative to the common commercial hydrophobic membranes due to their great features. However, these membranes are riddled with difficulties such as low spinning rate, use of high-risk and dangerous solvents, lower mechanical properties in the form of a neat fibrous structure, and fabricating membranes using expensive polymers. Therefore, a facile, cost-effective, and sustainable route was proposed to prepare hydrophobic nanofibrous membranes by simultaneously using inexpensive SAN polymer, a productive electroblowing process, and a low-toxic DMSO solvent. The nanofibrous SAN membranes fabricated by DMSO solvent were comparable with a SAN membrane fabricated by DMF solvent in the case of surface hydrophobicity, mechanical properties, and DCMD performance. The cold-pressing process was successfully used to improve mechanical robustness and endowed SAN membranes with high enough wetting resistance. Cold-pressed SAN/DMSO nanofibrous membranes demonstrated excellent salt rejection and higher permeate flux than that of commercial PTFE membranes when used to desalinate 35 g/L salty water. Overall, SAN/DMSO membranes are good competitors for state-of-the-art MD membranes considering their productivity, low cost, and desirable DCMD desalination performance.

CRediT authorship contribution statement

A. S. Niknejad: Data curation; Roles/Writing - original draft; Formal analysis; Conceptualization.
M. Pishnamazi: Writing – review & editing; Visualization.
S. Bazgir: Supervision; Methodology.
A. Kargari: Supervision; Methodology; Writing – review & editing.
M. M. A. Shirazi: Writing – original draft; Writing – review & editing.
M. Rasouli: Resources; Visualization.

Funding

This research did not receive any specific grant from funding agencies in the public, commercial, or not-for-profit sectors.

Declaration of Competing Interest

The authors declare that they have no known competing financial interests or personal relationships that could have appeared to influence the work reported in this paper.

Acknowledgments

The authors would like to appreciate the great support of Mr. Esmaeil Ranjbari and Mr. Masoud Barani during our test conducted in NPRL.

Data Availability

Data are available upon request.

References

[1] P.S. Goh, M.H.D. Othman, T. Matsuura, Waste Reutilization in Polymeric Membrane Fabrication: A New Direction in Membranes for Separation, Membranes 11 (2021) 782. https://doi.org/10.3390/membranes11100782.
[2] F. Zhu, Y.M. Zheng, B.G. Zhang, Y.R. Dai, A critical review on the electrospun nanofibrous membranes for the adsorption of heavy metals in water treatment, J. Hazard. Mater. 401 (2021) 123608. https://doi.org/10.1016/j.jhazmat.2020.123608.
[3] E. Ranjbari, S. Bazgir, M.M.A. Shirazi, Needleless electrospinning of poly (acrylic acid) superabsorbent: Fabrication, characterization and swelling behavior, Polym. Test. 84 (2020) 106403. https://doi.org/10.1016/j.polymertesting.2020.106403.
[4] M.M.A. Shirazi, A. Kargari, S. Ramakrishna, J. Doyle, M. Rajendrian, R. Babu, Electrospun membranes for desalination and water/wastewater treatment: a comprehensive review, J. Membr. Sci. Res. 3 (2017) 209–227. https://doi.org/10.22079/JMSR.2016.22349.
[5] P. Zahedi, I. Rezaeian, S.O. Ranaei-Siadat, S.H. Jafari, P. Supaphol, A review on wound dressing with an emphasis on electrospun nanofibrous polymeric bandages, Polym. Adv. Technol. 21 (2010) 77–95. https://doi.org/10.1002/pat.1625.
[6] X. Hu, S. Liu, G. Zhou, Y. Huang, Z. Xie, X. Jing, Electrospinning of polymeric nanofibers for drug delivery applications, J. Contr. Release 185 (2014) 12–21. https://doi.org/10.1016/j.jconrel.2014.04.018.
[7] H. Ke, M. Feldman, P. Guzman, J. Cole, Q. Wei, B. Chu, A. Alkhudhiri, R. Alrasheed, B.S. Hsiao, Electrospun polystyrene nanofibrous membranes for direct contact membrane distillation, J. Membr. Sci. 515 (2016) 86-97. https://doi.org/10.1016/j.memsci.2016.05.052.
[8] L.D. Tijing, Y.C. Woo, M.A.H. Johir, J.S. Choi, H.K. Shon, A novel dual-layer bicomponent electrospun nanofibrous membrane for desalination by direct contact membrane distillation, Chem. Eng. J. 256 (2014) 155–159. https://doi.org/10.1016/j.cej.2014.06.076.
[9] C. Feng, K.C. Khulbe, T. Matsuura, R. Gopal, S. Kaur, S. Ramakrishna, M. Khayet, Production of drinking water from saline water by air-gap membrane distillation using polyvinylidene fluoride nanofiber membrane, J. Membr. Sci. 311 (2008) 1-6. https://doi.org/10.1016/j.memsci.2007.12.026.
[10] M. Khayet, R. Wang, Mixed Matrix Polytetrafluoroethylene/Polysulfone Electrospun Nanofibrous Membranes for Water Desalination by Membrane Distillation, ACS Appl. Mater. Interfaces 10 (2018a) 24275-24287. https://doi.org/10.1021/acsami.8b06792.
[11] Z. Ma, M. Kotaki, S. Ramakrishna, Electrospun cellulose nanofiber as affinity membrane, J. Membr. Sci. 265 (2005) 115–123. https://doi.org/10.1016/j.memsci.2005.04.044.
[12] M. Khayet, M.C. Garcia-Payo, L. Garcia-Fernandez, J. Contreras-Martinez, Dual-layered electrospun nanofibrous membranes for membrane distillation, Desalination 426 (2018b) 174-184. https://doi.org/10.1016/j.desal.2017.10.036.
[13] X. Li, C. Wang, Y. Yang, X. Wang, M. Zhu, B.S. Hsiao, Dual-biomimetic superhydrophobic electrospun polystyrene nanofibrous membranes for membrane distillation, ACS Appl. Mater. Interf. 6 (2014) 2423–2430, https://doi.org/10.1021/am4048128.
[14] H.C. Duong, D. Chuai, Y.C. Woo, H.K. Shon, L.D. Nghiem, V. Sencadas, A novel electrospun, hydrophobic, and elastomeric styrene-butadiene-styrene membrane for membrane distillation applications, J. Membr. Sci. 549 (2018) 420-427. https://doi.org/10.1016/j.memsci.2017.12.024.

[15] Y. Liao, R. Wang, A.G. Fane, Engineering superhydrophobic surface on poly (vinylidene fluoride) nanofiber membranes for direct contact membrane distillation, J. Membr. Sci. 440 (2013) 77–87. https://doi.org/10.1016/j.memsci.2013.04.006.
[16] M. Wortmann, N. Frese, L. Sabantina, R. Petkau, F. Kinzel, A. Gölzhäuser, E. Moritzer, B. Hüsgen, A. Ehrmann, New Polymers for Needleless Electrospinning from Low-Toxic Solvents, Nanomaterials 9 (2019) 52. https://doi.org/10.3390/nano9010052.
[17] W. Xie, T. Li, C. Chen, H. Wu, S. Liang, H. Chang, B. Liu, E. Drioli, Q. Wang, J.C. Crittenden, Using the Green Solvent Dimethyl Sulfoxide To Replace Traditional Solvents Partly and Fabricating PVC/PVC-g-PEGMA Blended Ultrafiltration Membranes with High Permeability and Rejection, Ind. Eng. Chem. Res. 58 (2019) 6413–6423. https://doi.org/10.1021/acs.iecr.9b00370.
[18] A. Figoli, T. Marino, S. Simone, E. Di Nicolò, X.M. Li, T. He, S. Tornaghi, E. Drioli, Towards non-toxic solvents for membrane preparation: a review, Green Chem. 16 (2014) 4034. https://doi.org/10.1002/chin.201441295.
[19] D.T.T. Nu, N.P. Hung, C.V. Hoang, B. Van der Bruggen, Preparation of an asymmetric membrane from sugarcane bagasse using DMSO as green solvent, Appl. Sci. 9 (2019) 3347. https://doi.org/10.3390/app9163347.
[20] Y. Mao, Q. Huang, B. Meng, K. Zhou, G. Liu, A. Gugliuzza, E. Drioli, W. Jin, Roughness-enhanced hydrophobic graphene oxide membrane for water desalination via membrane distillation, J. Membr. Sci. 611 (2020) 118364. https://doi.org/10.1016/j.memsci.2020.118364.
[21] S. Zare, A. Kargari, Membrane properties in membrane distillation. In Emerging Technologies for Sustainable Desalination Handbook, 107-156 (2018). https://doi.org/10.1016/B978-0-12-815818-0.00004-7.
[22] A. Alkhudhiri, N. Darwish, N. Hilal, Membrane distillation: A comprehensive review, Desalination 287 (2012) 2-18. https://doi.org/10.1016/j.desal.2011.08.027.
[23] M. Khayet, Membranes and theoretical modeling of membrane distillation: A review, Adv. Colloid Interf. Sci. 164 (2011) 56-88. https://doi.org/10.1016/j.cis.2010.09.005.
[24] L. Eykens, K. De Sitter, C. Dotremont, L. Pinoy, B. Van der Bruggen, How to optimize the membrane properties for membrane distillation: A review, Ind. Eng. Chem. Res. 55 (2016a) 9333-9343. https://doi.org/10.1021/acs.iecr.6b02226.
[25] L. Eykens, K. De Sitter, C. Dotremont, L. Pinoy, B. Van der Bruggen, Membrane synthesis for membrane distillation: A review, Sep. Purif. Technol. 182 (2017) 36-51. https://doi.org/10.1016/j.seppur.2017.03.035.
[26] K. Gethard, O. Sae-khow, S. Mitra, Carbon nanotube enhanced membrane distillation for simultaneous generation of pure water and concentrating pharmaceutical waste, Sep. Purif. Technol. 90 (2012) 239-245. https://doi.org/10.1016/j.seppur.2012.02.042.
[27] F. Li, J. Huang, Q. Xia, M. Lou, B. Yang, Q. Tian, Y. Liu, Direct contact membrane distillation for the treatment of industrial dyeing wastewater and characteristic pollutants, Sep. Purif. Technol. 195 (2018) 83–91. https://doi.org/10.1016/j.seppur.2017.11.058.
[28] S. Leaper, A. Abdel-Karim, T.A. Gad-Allah, P. Gorgojo, Air-gap membrane distillation as a one-step process for textile wastewater treatment, Chem. Eng. J. 360 (2019) 1330–1340. https://doi.org/10.1016/j.cej.2018.10.209.
[29] H. Liu, J. Wang, Treatment of radioactive wastewater using direct contact membrane distillation, J. Hazard. Mater. 261 (2013) 307–315. https://doi.org/10.1016/j.jhazmat.2013.07.045.
[30] M. Khayet, Treatment of radioactive wastewater solutions by direct contact membrane distillation using surface-modified membranes, Desalination, 321 (2013) 60–66. https://doi.org/10.1016/j.desal.2013.02.023.
[31] P. Zhang, P. Knötig, S. Gray, M. Duke, Scale reduction and cleaning techniques during direct contact membrane distillation of seawater reverse osmosis brine, Desalination 374 (2015) 20–30. https://doi.org/10.1016/j.desal.2015.07.005.
[32] C. Su, C. Lu, H. Cao, K. Tang, J. Chang, F. Duan, X. Ma, Y. Li, Fabrication and post-treatment of nanofibers-covered hollow fiber membranes for membrane distillation, J. Membr. Sci. 56 (2018) 38–46. https://doi.org/10.1016/j.memsci.2018.05.027.
[33] M. Gryta, Long-term performance of membrane distillation process, J. Membr. Sci. 265 (2005) 153-159. https://doi.org/10.1016/j.memsci.2005.04.049.
[34] B.L. Pangarkar, M.G. Sane, S.B. Parjane, M. Guddad, Status of membrane distillation for water and wastewater treatment-A review, Desal. Water Treat. 52 (2014) 5199-5218. https://doi.org/10.1080/19443994.2013.808422.
[35] N. Thomas, M.O. Mavukkandy, S. Loutatidou, H.A. Arafat, Membrane distillation research & implementation: Lessons from the past five decades, Sep. Purif. Technol. 189 (2017) 108-127. https://doi.org/10.1016/j.seppur.2017.07.069.
[36] L.N. Nthunya, L. Gutierrez, S. Derese, E.N. Nxumalo, A.R. Verliefde, B.B. Mamba, S.D. Mhlanga, A review of nanoparticle-enhanced membrane distillation membranes: membrane synthesis and applications in water treatment, J. Chem. Technol. Biotechnol. 94 (2019) 2757-2771. https://doi.org/10.1002/jctb.5977.
[37] J. Kim, Recent progress on improving the sustainability of membrane fabrication, J. Membr. Sci. Res. 6 (2020) 241-250. https://doi.org/10.22079/JMSR.2019.106501.1260.
[38] R. Aminyan and S. Bazgir, Fabrication and characterization of nanofibrous polyacrylic acid superabsorbent using gas-assisted electrospinning technique, React Funct Polym 141 (2019) 133–144. https://doi.org/10.1016/j.reactfunctpolym.2019.05.012.
[39] A. Sadeghzadeh, S. Bazgir, M.M.A. Shirazi, Fabrication and characterization of a novel hydrophobic polystyrene membrane using electroblowing technique for desalination by direct contact membrane distillation, Sep. Purif. Technol. 239 (2020) 116498. https://doi.org/10.1016/j.seppur.2019.116498.
[40] M.M.A. Shirazi, S. Bazgir, F. Meshkani, A novel dual-layer, gas-assisted electrospun, nanofibrous SAN4-HIPS membrane for industrial textile wastewater treatment by direct contact membrane distillation (DCMD), J. Water Process. Eng. 36 (2020) 101315. https://doi.org/10.1016/j.jwpe.2020.101315.
[41] A.S. Niknejad, S. Bazgir, M. Ardjmand, M.M.A Shirazi, Spent caustic wastewater treatment using direct contact membrane distillation with electroblown styrene-acrylonitrile membrane, Int. J. Environ. Sci. Technol. (2020a) 1-12. https://doi.org/10.1007/s13762-020-02972-x.
[42] A. Haider, S. Haider, I.K. Kang, A comprehensive review summarizing the effect of electrospinning parameters and potential applications of nanofibers in biomedical and biotechnology, Arab. J. Chem. 11 (2018) 1165-1188. https://doi.org/10.1016/j.arabjc.2015.11.015.
[43] T. Jarusuwannapoom, W. Hongrojjanawiwat, S. Jitjaicham, L. Wannatong, M. Nithitanakul, C. Pattamaprom, P. Koombhongse, R. Rangkupan, P. Supaphol, Effect of solvents on electro-spinnability of polystyrene solutions and morphological appearance of resulting electrospun polystyrene fibers. European Polymer Journal, 41 (2005) 409-421. https://doi.org/10.1016/j.eurpolymj.2004.10.010.
[44] M. Sazegar, S. Bazgir, A.A. Katbab, Preparation and characterization of water-absorbing gas-assisted electrospun nanofibers based on poly(vinyl alcohol)/chitosan, Mater. Today Commun. 25 (2020) 101489. https://doi.org/10.1016/j.mtcomm.2020.101489.
[45] J. Prince, G. Singh, D. Rana, T. Matsuura, V. Anbharasi, T. Shanmugasundaram, Preparation and characterization of highly hydrophobic poly(vinylidene fluoride)– Clay nanocomposite nanofiber membranes (PVDF–clay NNMs) for desalination using direct contact membrane distillation, J. Membr. Sci. 397-398 (2012) 80-86. https://doi.org/10.1016/j.memsci.2012.01.012.
[46] K.J. Lu, J. Zuo, J. Chang, H.N. Kuan, T.S. Chung, Omniphobic Hollow-Fiber Membranes for Vacuum Membrane Distillation, Environ. Sci. Technol. 52 (2018) 4472-4480. https://doi.org/10.1021/acs.est.8b00766.
[47] E.J. Lee, A.K. An, T. He, Y.C. Woo, H.K. Shon, Electrospun nanofiber membranes incorporating fluorosilane-coated TiO2 nanocomposite for direct contact membrane distillation, J. Membr. Sci. 520 (2016) 145-154. https://doi.org/10.1016/j.memsci.2016.07.019.
[48] A.S. Niknejad, S. Bazgir, A. Sadeghzadeh, M.M.A. Shirazi, Styrene-acrylonitrile (SAN) nanofibrous membranes with unique properties for desalination by direct contact membrane distillation (DCMD) process, Desalination 488 (2020b) 114502. https://doi.org/10.1016/j.desal.2020.114502.
[49] F. Russo, C. Ursino, E. Avruscio, G. Desiderio, A. Perrone, S. Santoro, F. Galiano, A. Figoli, Innovative Poly (Vinylidene Fluoride) (PVDF) Electrospun Nanofiber Membrane Preparation Using DMSO as a Low Toxicity Solvent. Membranes, 10 (2020) 36. https://doi.org/10.3390/membranes10030036.
[50] Smallwood, I.M. Solvent Recovery Handbook, 2nd ed.; CRC Press: Boca Raton, FL, USA, 2002; p. 13.
[51] L. Eykens, I. Hitsov, K. De Sitter, C. Dotremont, L. Pinoy, I. Nopens, B. Van der Bruggen, Influence of membrane thickness and process conditions on direct contact membrane distillation at different salinities, J. Membr. Sci. 498 (2016b) 353–364. https://doi.org/10.1016/j.memsci.2015.07.037.
[52] M. Yao, Y.C. Woo, L.D. Tijing, W.G. Shim, J.S. Choi, S.H. Kim, H.K. Shon, Effect of heat-press conditions on electrospun membranes for desalination by direct contact membrane distillation, Desalination 378 (2016) 80–91. https://doi.org/10.1016/j.desal.2015.09.025.
[53] M.M.A. Shirazi, A. Kargari, M. Tabatabaei, Evaluation of commercial PTFE membranes in desalination by direct contact membrane distillation, Chem. Eng. Proc.: Process Intensif. 76 (2014) 16–25. https://doi.org/10.1016/j.cep.2013.11.010.

[54] M.S. El-Bourawi, Z. Ding, R. Ma, M. Khayet, A framework for better understanding membrane distillation separation process, J. Membr. Sci. 285 (2006) 4–29. https://doi.org/10.1016/j.memsci.2006.08.002.

[55] H. Attia, D.J. Johnson, C.J. Wright, N. Hilal, Robust superhydrophobic electrospun membrane fabricated by combination of electrospinning and electrospraying techniques for air gap membrane distillation, Desalination 446 (2018) 70–82. https://doi.org/10.1016/j.desal.2018.09.001.

[56] M. Essalhi, M. Khayet, Self-sustained webs of polyvinylidene fluoride electrospun nano-fibers: effects of polymer concentration and desalination by direct contact membrane distillation, J. Membr. Sci. 454 (2014) 133–143. http://dx.doi.org/10.1016/j.memsci.2013.11.056.

[57] M. Essalhi, M. Khayet, Self-sustained webs of polyvinylidene fluoride electrospun nanofibers at different electrospinning times: 1. Desalination by direct contact membrane distillation, J. Membr. Sci. 433 (2013) 167–179. https://doi.org/10.1016/j.memsci.2013.01.023.

[58] Z. Wang, J. Jin, D. Hou, S. Lin, Tailoring surface charge and wetting property for robust oil-fouling mitigation in membrane distillation, J. Membr. Sci. 518 (2016) 113-122. https://doi.org/10.1016/j.memsci.2016.06.011.

[59] C. Su, C. Lu, T. Horseman, H. Cao, F. Duan, L. Li, M. Li, Y. Li, Dilute solvent welding: A quick and scalable approach for enhancing the mechanical properties and narrowing the pore size distribution of electrospun nanofibrous membrane. J. Membr. Sci. 595 (2020) 117548. https://doi.org/10.1016/j.memsci.2019.117548.

[60] J. Xu, Y.B. Singh, G.L. Amy, N. Ghaffour, Effect of operating parameters and membrane characteristics on air gap membrane distillation performance for the treatment of highly saline water, J. Membr. Sci. 512 (2016) 73–82. https://doi.org/10.1016/j.memsci.2016.04.010.

[61] B.S. Lalia, E. Guillen-Burrieza, H.A. Arafat, R. Hashaikeh, Fabrication and characterization of polyvinylidene fluoride-co-hexafluoropropylene (PVDF-HFP) electrospun membranes for direct contact membrane distillation. Membr. Sci. 428 (2013) 104–115. https://doi.org/10.1016/j.memsci.2012.10.061.